

# Optical Coherence Microrheology: Imaging Tissue Viscoelastic Properties

Amy L. Oldenburg

Department of Physics and Astronomy and the Biomedical Research Imaging Center,  
University of North Carolina at Chapel Hill, Phillips Hall, Chapel Hill, NC 27599-3255, USA  
[aold@physics.unc.edu](mailto:aold@physics.unc.edu)

**Abstract:** Volumetric imaging of tissue mechanical properties using active probes (magnetic nanoparticles) and passive probes (plasmon-resonant gold nanorods) by processing signals obtained using optical coherence tomography provides a new window into tissue mechanics. OCIS codes: (110.4500) Optical coherence tomography; (290.1990) Diffusion

## 1. Introduction

Microrheology is of growing interest for probing localized viscoelastic properties in and around cells by monitoring diffusive (passive) motion or induced (active) motion of micro- and nanoprobe [1]. Current microrheological techniques predominantly rely upon single-particle tracking via microscopy, or diffusing wave spectroscopy through turbid media. The former provides excellent spatial resolution but limited depth penetration, while the latter provides viscoelastic properties over large depths but with poor spatial resolution. Optical coherence tomography (OCT), due to its ability to path-length resolve dynamic light scattering [2,3], can potentially mitigate these limitations by providing local microrheological properties in turbid media, dubbed “optical coherence microrheology (OCMR).

OCMR is particularly advantageous because 1) phase-resolved imaging is sensitive to nanoscale probe motions, and 2) the collective or diffusive motion of ensembles of nanoparticles detected within each coherence volume provide good statistical averaging in a short acquisition time. Recently, the ability to spatially map the diffusion rate of microspheres using spectral-domain OCT was demonstrated [4]. However, important considerations remain before applying OCMR to tissues, including 1) the ability to relate the probe motions to the desired viscoelastic tissue properties, and 2) the ability to separate the probe optical signal from that of the endogenous tissue scatterers. Below I address these considerations while outlining two promising techniques for OCMR based upon passive (diffusive) and active (magnetically-actuated) nanoprobe.

## 2. Passive OCMR using Plasmon-Resonant Gold Nanorods

OCMR can be performed by sensing the passive (Brownian) rotational diffusion of nanorods [5]. Plasmon-resonant gold nanorods (GNRs) provide highly polarized optical scattering at their longitudinal resonance mode, which has previously been used to sense their orientation [6]. When diffusing in fluids, the Brownian tumbling of GNRs results in a fluctuating cross-polarized scattered electric field,  $E_{HV}(t)$ . As described previously [5], the cross-polarized (HV) OCT signal is related to the first-order correlation function of the field,  $g_{HV}^{(1)}(z, \tau)$ . For GNRs small compared to the wavelength,  $g_{HV}^{(1)}$  is determined by the rotational diffusion of GNRs according to:

$g_{HV}^{(1)}(z, \tau) \propto e^{-6D_R(z)\tau}$ , where  $D_R(z)$  is the depth ( $z$ )-resolved rotational diffusion of GNRs. As such, an OCT axial line scan can be repeated over sufficiently long time, cross-correlated at each depth, fit to an inverse exponential, and the diffusion rate subsequently determined by the decay time  $\tau_{1/e}$  according to  $D_R(z) = 1/(6\tau_{1/e})$ .

The ability to perform OCMR, then, depends upon application of an appropriate Stokes-Einstein relationship to connect  $D_R(z)$  to viscosity  $\eta(z)$  in Newtonian fluids. (In future work, a generalized relationship can be used to map the frequency-dependent shear modulus  $G(\omega)$ , which contains both viscous (loss) and elastic (storage) components, to describe arbitrary non-Newtonian fluids). The Stokes drag force on GNRs is proportional to  $\eta$ , such that  $D_R \propto 1/\eta$ . Calibration of GNRs in fluids of known viscosity is used to determine the proportionality constant, and to generate maps of  $\eta(z)$  in an arbitrary sample object. This is demonstrated in Fig. 1, which shows an M-mode (repetitive axial scan) OCT image of a double chamber containing GNRs in solutions of different viscosities, and the resulting processed image of depth-resolved viscosity  $\eta(z)$ , which is well-matched to the actual viscosities in each chamber.

GNRs have a rapidly fluctuating, cross-polarized signal, which may be separable from less anisotropic and more slowly moving scatterers that are endogenous to tissue. However, future work is needed to determine whether interference from tissue scattering is significant and, if so, how to separate them from that from the GNRs.

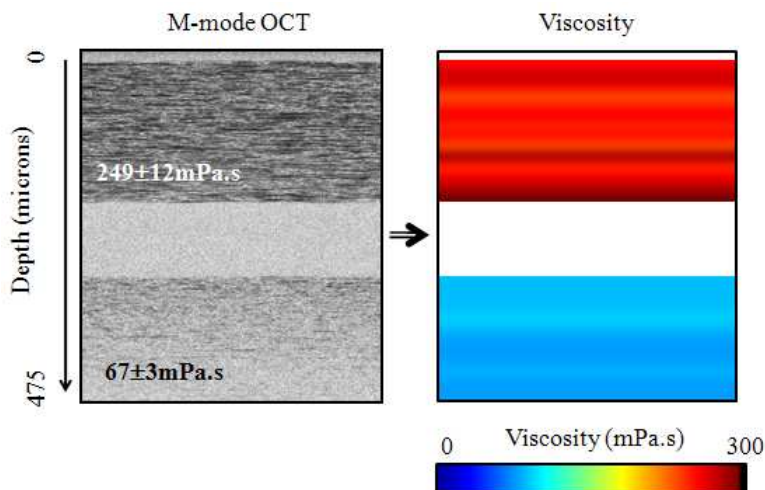


Fig. 1. (Left): M-mode OCT of GNRs in two chambers of different viscosities separated by a coverslip (low scattering region in the center), and (right) computed viscosity versus depth within the chambers.

### 3. Active OCMR using Magnetic Nanoparticles

Unlike GNRs, the optical signal derived from magnetic nanoparticles under magnetic field modulation has been proven to be separable from that of endogenous tissue [7]. This is based upon the difference in magnetic susceptibility between weak, diamagnetic tissues and that of strong, superparamagnetic iron oxide nanoparticles (SPIOs). However, also unlike GNRs, the ability to relate magnetically-induced SPIO motion to viscoelastic tissue properties is not straightforward. As such, there are pros and cons to each of these techniques.

Active OCMR is based upon sensing induced motions of SPIOs diffused into tissues and subsequently pulled on using a magnetic gradient field. In this scenario, the force per volume is given by:  $\frac{F}{V} = \left( (m_p N_p + M_t) \cdot \nabla \right) B$

where  $N_p$  is the local number density of nanoparticles,  $m_p$  is the magnetization per particle,  $M_t$  is the volume magnetization of the tissue surrounding the particles, and  $B$  is the magnetic field. This induces a stress field which results in elastic tissue deformation (a strain field) that is measured as a phase shift in the OCT interferogram:  $\Delta\phi = 4\pi\Delta z/\lambda$ , where  $\Delta z$  is the axial displacement at each location in the tissue. With the use of well-defined boundary conditions and a homogeneous distribution of SPIOs, it is possible to determine the elastic modulus of the tissue by comparison of the known stress to measured strain fields. However, because  $\Delta z$  is both proportional to the SPIO concentration  $N_p$ , and inversely proportional to the elastic modulus, future work is needed to determine the information available in tissues with heterogeneous distributions of SPIOs.

### 4. References

- [1] T. M. Squires and T. G. Mason, "Fluid mechanics of microrheology," *Annu. Rev. Fluid Mech.* **42**, 413-438 (2010).
- [2] D. A. Boas, K. K. Bizheva, and A. M. Siegel, "Using dynamic low-coherence interferometry to image Brownian motion within highly scattering media," *Opt. Lett.* **23**, 319-321 (1998).
- [3] A. Wax, C. Yang, R. R. Dasari, and M. S. Feld, "Path-length-resolved dynamic light scattering: modeling the transition from single to diffusive scattering," *Appl. Opt.* **40**, 4222-4227 (2001).
- [4] J. Kalkman, R. Spirik, T. G. van Leeuwen, "Path-length-resolved diffusive particle dynamics in spectral-domain optical coherence tomography," *Phys. Rev. Lett.* **105**, 198302 (2010).
- [5] R. K. Chhetri, K. A. Kozek, A. C. Johnston-Peck, J. B. Tracy, and A. L. Oldenburg, "Imaging three-dimensional rotational diffusion of plasmon-resonant gold nanorods using polarization-sensitive optical coherence tomography," *Phys. Rev. E* **83**, 040903(R) (2011).
- [6] C. Sonnichsen and A. P. Alivisatos, "Gold nanorods as novel nonbleaching plasmon-based orientation sensors for polarized single-particle microscopy," *Nano Lett.* **5**, 301-304 (2005).
- [7] A. L. Oldenburg, V. Crecea, S. A. Rinne, and S. A. Boppart, "Phase-resolved magnetomotive OCT for imaging nanomolar concentrations of magnetic nanoparticles in tissues," *Opt. Express* **16**, 11525-11539 (2008).